Graphite-loaded cotton wool: A green route to highly-porous and solid graphite pellets for thermoelectric devices

Rafiq Mulla, Charles W. Dunnill

PII: S2452-2139(20)30067-X

DOI: https://doi.org/10.1016/j.coco.2020.04.011

Reference: COCO 345

To appear in: *Composites Communications*

Received Date: 10 March 2020

Revised Date: 16 April 2020

Accepted Date: 19 April 2020

Please cite this article as: R. Mulla, C.W. Dunnill, Graphite-loaded cotton wool: A green route to highly-porous and solid graphite pellets for thermoelectric devices, *Composites Communications* (2020), doi: https://doi.org/10.1016/j.coco.2020.04.011.

Rafiq Mulla: Conceptualization, Methodology, Writing- Original draft preparation, Investigation.

Charles W. Dunnill: Supervision, Writing- Reviewing and Editing, Resources, Project administration, Funding acquisition

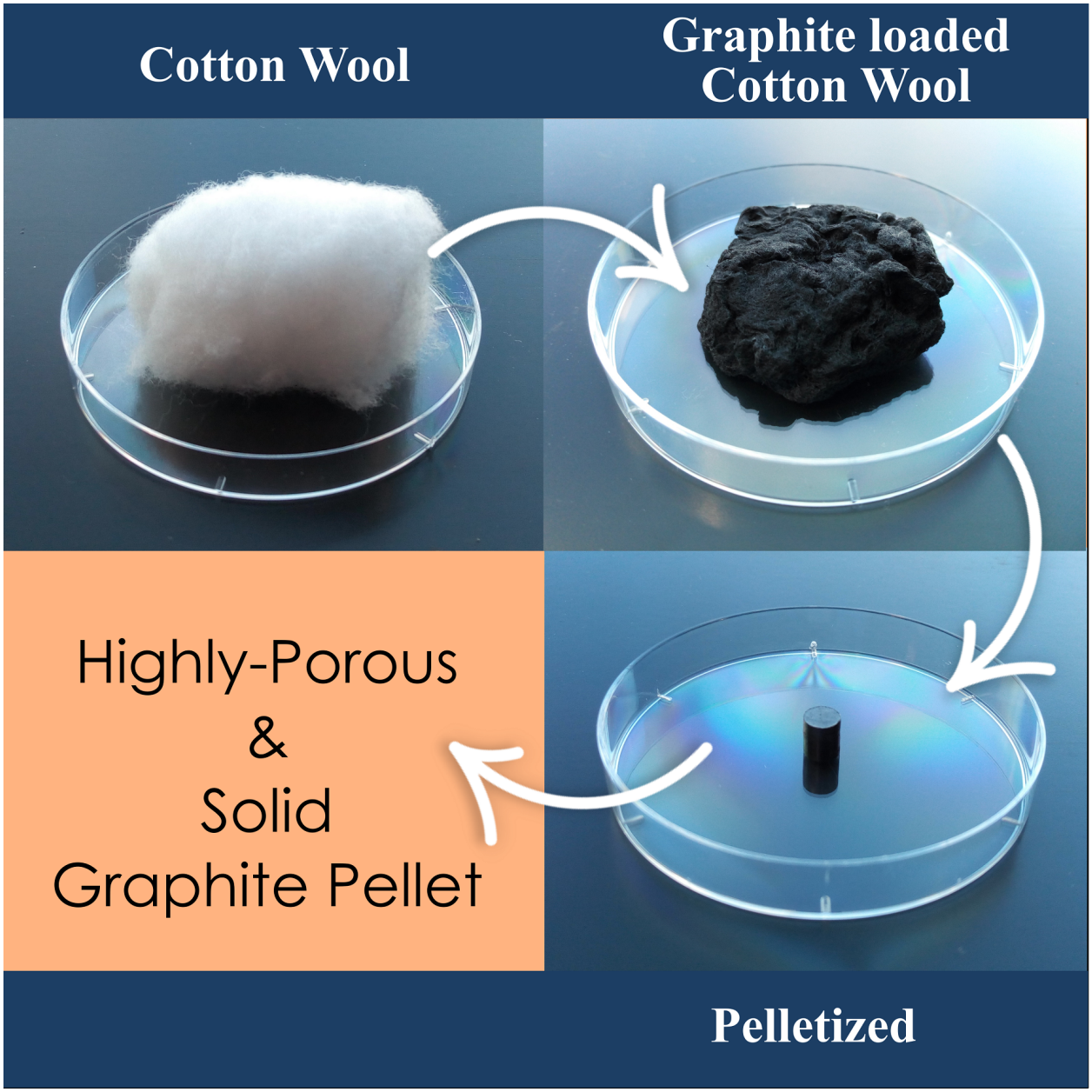
Cotton Wool
Graphite loaded Cotton Wool
Highly-Porous & Solid Graphite Pellet
Pelletized

Graphite-Loaded Cotton Wool: A Green Route to Highly-Porous and Solid Graphite Pellets for Thermoelectric Devices

Rafiq Mulla and Charles W. Dunnill*

Energy Safety Research Institute, Swansea University, Bay Campus, Fabian Way, SA1 8EN, UK.

Abstract:

The high porosity of thermoelectric materials is a valuable feature to ideally reduce thermal conductivity without degrading electrical conductivity. This paper describes a unique low-temperature and direct method for making highly porous yet solid graphite pellets. Cotton wools were loaded with graphite particles, and pressed to yield low-density graphite pellets. The electrical and thermal properties of the resulting pellets have been studied. A significant reduction in the heat flow through the pellets has been observed as compared to a pure graphite pellet. For the porous pellets, the electrical conductivity was slightly lower than that of pure graphite pellets due to the charge scattering processes of the highly porous network, yet the thermal conductivity was drastically reduced with enhancements in Seebeck coefficients hence, a significant improvement in the thermoelectric property. Overall, the power factor was found to increase from 0.303 $\mu Wm^{-1}K^{-2}$ for solid graphite pellet to 0.424 $\mu Wm^{-1}K^{-2}$ for porous graphite pellet, showing a simultaneously improved power factor and reduced thermal conductance. The approach can be extended for other good thermoelectric materials to achieve further enhancements in their properties and useful to reduce material cost.

Keywords: Thermoelectric; porous graphite; green method; cotton wool fibres.

*Corresponding Author E-mail address: c.dunnill@swansea.ac.uk

Tel: +44 (0)1792 606244

1. Introduction

Thermoelectric devices convert a thermal gradient (heat) into an electric charge and have numerous applications across a wide range of industries including the scavenging of waste industrial thermal energy.[1] Key to their performance is the ability to conduct electricity well but heat poorly. Achieving lower density in materials is often an important objective in thermoelectrics as increasing the porosity in the materials tends to have advantages in scattering phonons at grain boundaries to helps in reducing thermal conductivity.[2] Therefore, intentionally introducing porosity into materials has become a strategy to improve thermoelectric performance by controlling their thermal conductivity.[3, 4] In theory, the porosity of material affects both electrical and thermal conductance, though there are possibilities of changing one parameter more than the other. Alternatively, porous thermoelectric legs can reduce the amount of material required to make modules.

Introducing pores into materials is found to be beneficial yet challenging to produce material in large quantity.[3] Different methodologies have been introduced to get porous thermoelectric materials, and it is observed that obtaining such porous structured materials is not straightforward.[3, 5, 6] Similarly, phonon scattering can be improved by introducing different types of scattering centres such as nano-microscale precipitates,[7, 8] interfaces,[9-11] hierarchical designs,[12, 13] nanostructuring,[1, 14] etc.

In this study, graphite powder has been chosen to fabricate its highly porous structured compacts for their possible applications in thermoelectrics. Graphite is an abundant and non-toxic material and is one of the cheapest electrically conducting materials. The material has shown exciting electrical and thermal properties especially when it is in two dimensional, popularly known as graphene.[15-18] Its very high thermal conductivity, however, has limited its use in the thermoelectric applications.[15] Studies exist, making such porous carbon compounds in the form of carbon aerogels,[19] carbon-ink or graphene-

coated polyurethanes,[20, 21] porous graphene,[22] carbon foams,[23-26] porous and hallow carbons[27-29] carbon-polymer composite foams,[30, 31] for different applications.[32, 33] Most of these products are highly porous, flexible and useful but sometimes delicate to handle. But typically, to make a solid-state thermoelectric device, the p-and-n-type thermoelectric elements/legs should be robust and solid for its successful working. Here, a direct method of making low-density, porous yet solid graphite pellets has been shown via a facile and green method performed at ambient conditions.

2. Materials and Methods

Graphite powder (99%) was obtained from Alfa Aeser and cotton wool balls were purchased from a local stationery store. Deionized water was used as a solvent to make graphite dispersion for the coating.

2.1. Preparing graphite dispersion in water

In order to improve the dispersion quality of graphite powder, it was ball milled under aqueous media. Graphite powder (2 g) was added to an 80 ml stainless steel grinding bowl, to which water (20 ml) and 200 stainless steel ball bearings (5 mm in diameter) were added to the bowl and the bowl was transferred into a planetary mill (Fritsch P6 Planetary Mono Mill). The mixture was milled at a speed of 300 rpm for 4 hr (cycles of 5 min milling followed by 2 min rest, repeated for 4 hr). The resulting black slurry-like product was dispersed into the water in a glass reagent bottle to make ~100 ml graphite dispersion.

2.2. Modifying cotton wool with graphite

To the above-prepared dispersion, a cotton wool ball (0.516 g) was added and held on a rotamixer (Hati Rotamixer Vortex Mixer) for 2 min. Finally, the black coloured cotton wool ball was taken out from the solution, squeezed to remove excess/lose graphite particles and water in it, and dried inside an oven at 60 ºC. The final weight of the wool was found to be 0.626 g, indicating 0.110 g of graphite in it. Approximately 0.1 g was carefully cut from the

above wool for the pelletization and pressed using a pellet press die set of 5 mm in diameter (load: 2 ton, pressing time: 5 min). The thickness of the resulting pellet (denoted as **CW1**) was 3.12 mm.

A similar process was followed to make another graphite-loaded cotton wool (initial weight of the wool was 0.504 g) using the same dispersion solution. Here, the dried graphite-loaded wool was gently tapped several times to remove loosely bound graphite particles from it and the final weight of the wool was found to be 0.591 g, showing 0.087 g of graphite in the wool. A pellet was made using similar conditions that were used for the first case. The thickness of the pellet (**CW2**) obtained from the ~0.1 g of wool was 3.20 mm. To make pellets with further lower graphite loading, a new graphite dispersion of low concentration (0.5 g graphite powder in 100 ml water) has been used that gave sample **CW3** and tapped graphite-loaded wool resulted in sample **CW4**. Further, to make a comparative study, a complete graphite powder-based pellet was made with similar pressing conditions. For that, a pellet of similar thickness was made to ease the comparison between this and **CW1** and **CW2** pellets, a pellet of thickness 3.30 mm was obtained using 0.125 g of graphite powder.

The morphologies of the cotton wool and graphite-loaded cotton wool and its pellet were obtained by Scanning Electron Microscopy (SEM) (Models: Joel 7800F FEG SEM and Zeiss Evo LS25 SEM) and an optical microscope.

2.3. Thermoelectric measurements and thermal gradient testing

Electrical and Seebeck coefficient measurements were conducted up to 100 ºC through a lab-built apparatus, described elsewhere[34], across the thickness of the pellets. Temperature-dependent Seebeck coefficients were obtained by measuring voltage developed from the sample under the application of temperature gradients across the pellets. The Seebeck coefficient values were estimated using the expression,

$$S = -\left(\frac{\Delta V}{\Delta T}\right) \qquad \text{……..(1)}$$

where ΔV is the voltage produced across the sample under an applied temperature gradient, ΔT. The resulting values were corrected with electrode contribution. The resistivity (ρ) of the pellets was measured using the standard two-probe method by passing a current (I) through the thickness and measuring resulting voltages (V), using the expression,

$$\rho = \frac{RA}{l} \qquad \text{.....(2)}$$

where $R=V/I$ is the resistance across the pellet, A is the cross-sectional area of the pellet, and l is the thickness of the pellet. The inverse of the resistivity values were estimated to get electrical conductivity (σ) of the samples. A comparative thermal property of the pellets was studied by means of temperature gradient estimation for all the samples. The thermal gradients produced across the pellets were measured as a function of time by heating one side of the pellet with a constant power supply to the heater.

3. Results and discussion

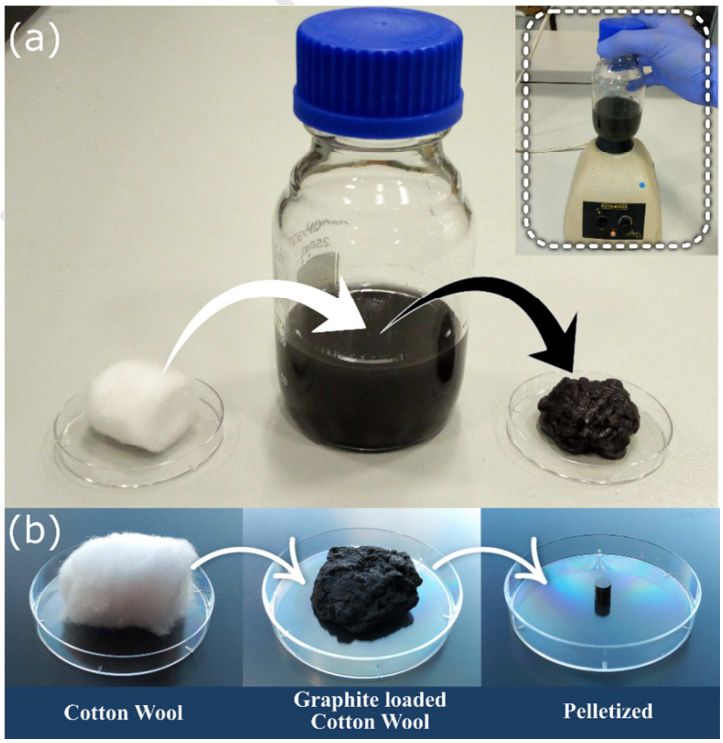

Figure 1. (a) A schematic illustrating the graphite loading process into cotton wool (inset shows the Rotamixer used for rapid shaking of the graphite dispersion) and (b) pictures of as received cotton wool, graphite-loaded cotton wool, and its pellet.

As shown by Figure 1, the process of graphite loading into cotton wool is quite straightforward. The real pictures of cotton wool, as prepared graphite-loaded cotton wool and its pressed pellet are shown in Figure 1 (b). More detailed pictures of the wool and pellet surface were captured using an optical microscope (Figure 2). A uniform coating of graphite on cotton fibres can be observed in Figures 2 (b). Figure 2 (d) shows pellets of complete graphite powder and one of the graphite-loaded cotton wool pellets to illustrate the dimensional similarity.

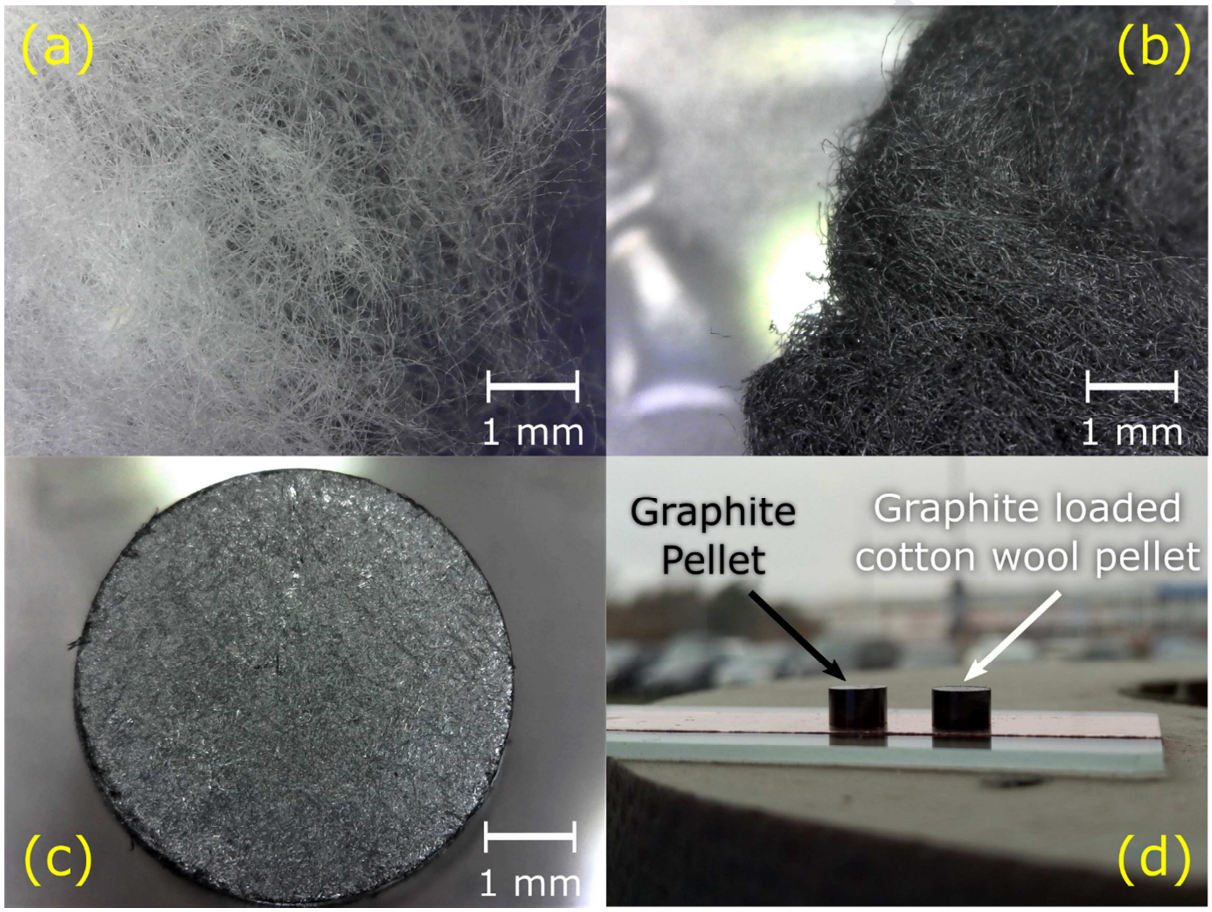

Figure 2. Optical microscope images of (a) cotton wool, (b) graphite-loaded cotton wool, (c) surface of the pressed pellet, and (d) is the picture showing graphite and graphite-loaded cotton wool pellets.

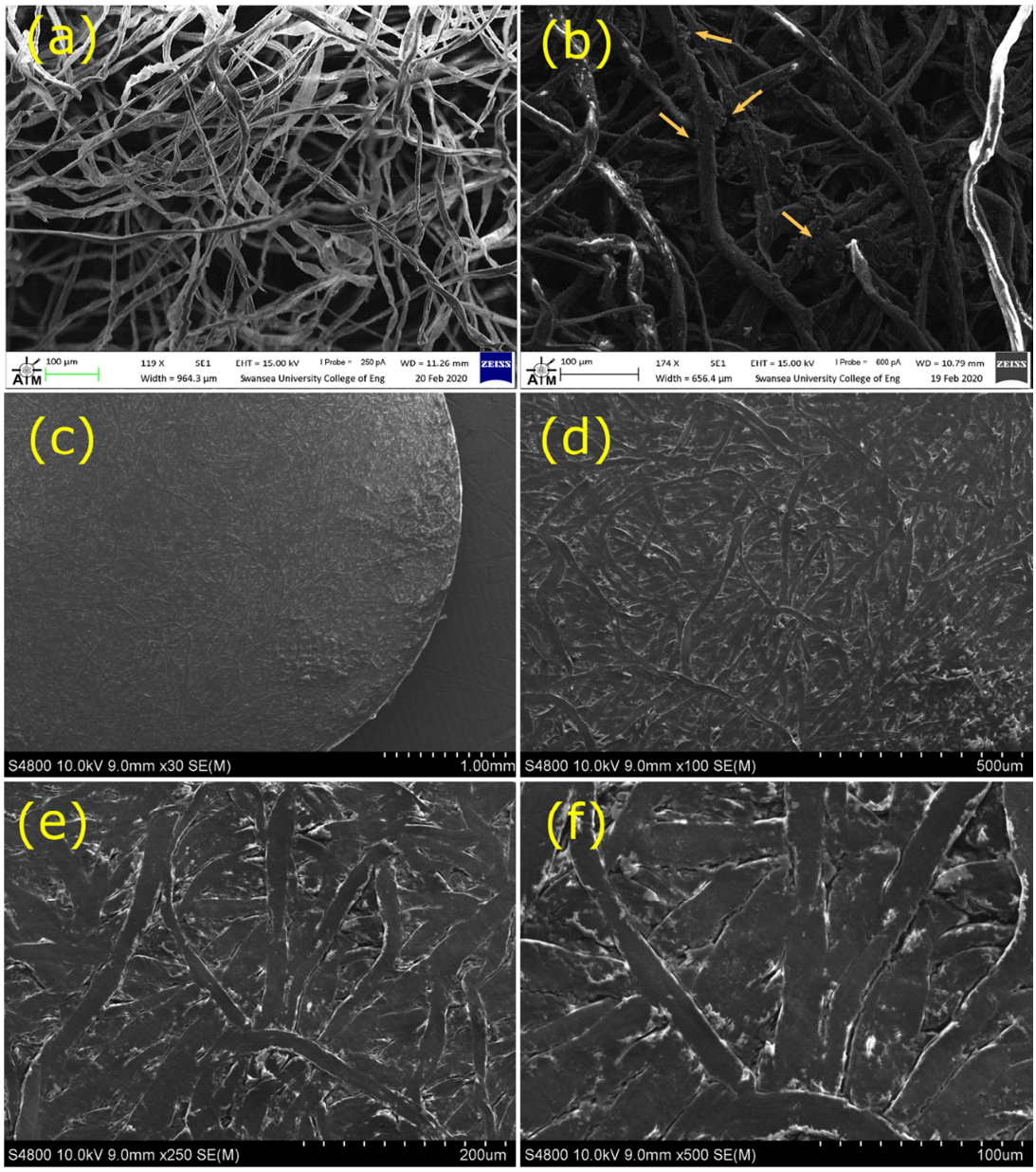

Figure 3. SEM images of (a) cotton wool fibres, (b) graphite-loaded cotton wool fibres, and (c-f) are SEM images the graphite-loaded cotton wool (**CW1**) pellet's surface with different magnifications.

Higher resolution images of cotton wool fibres have been obtained by the SEM instrument are shown in Figure 3. Figure 3 (a) and (b) show uncoated and graphite-coated fibres, respectively. The graphite loading or coating can be seen from comparing the two images. The arrows in Figure 3 (b) show some of the bulk graphite particles residing on the fibre networks. Figure 3 (c-f) give SEM images of one of the pellet's (**CW1**) surface with different

magnifications. Compact and well-connected graphite coated fibres can be seen from the surface of the pellets. The SEM images of the uncoated cotton fibre, graphite coated fibres of **CW1** and **CW2** samples and raw graphite particles used are shown in Figure S1 of the Supplementary material.

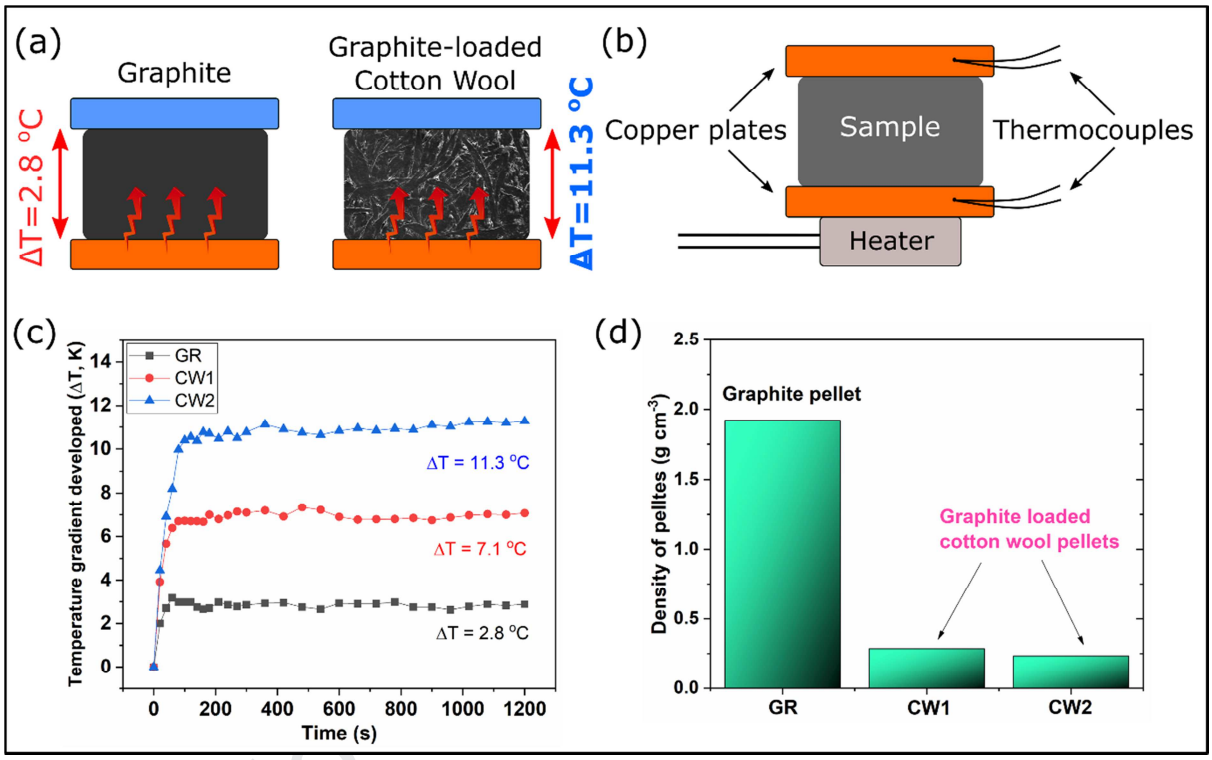

Figure 4. Schematic of the measurement method used to estimate thermal gradients across the samples and observed temperature gradients across graphite (**GR**) and **CW2** pellets (a-b), (c) shows the data of temperature gradient (ΔT) obtained from the graphite (**GR**), **CW1**, and **CW2** pellets as a function of time, and (d) gives the graphite density values of the pellets used in the work.

To investigate the thermal properties of the graphite (**GR**), **CW1**, and **CW2** pellets, a thermal gradient test has been performed. The data of temperature gradient (ΔT) obtained from the samples as a function of time has been plotted in Figure 4 (c). The variations in the temperatures at the hot side and cold side of the pellets were recorded up to 20 min at which near-saturated temperatures were observed, the data is used to estimate temperature gradients

at different times. The maximum and stable temperature gradient across the graphite pellet observed after 20 min was 2.8 ºC, whereas significantly improved values were seen from **CW1** and **CW2** pellets, recording maximum gradients of 7.1 ºC and 11.3 ºC, respectively. Figures 4 (a-b) shows a schematic of the measurement method used to estimate thermal gradients across the samples. Such an increase in the ΔT in **CW1** and **CW2** can be understood from the fact that they have highly structured and porous graphitic networks in them due to the presence of a high volume of wool fibres. The possible reason behind the improved thermal properties is the scattering mechanism of both phonons and electrons from the porous nature/multiple interfaces that are created due to the presence of cotton fibres in the medium. But, in case of bulk graphite these carriers do not have such extra scattering regions and hence they can flow without being scattered. In addition, the thermal conductivity of the cotton is very low (<0.065 $Wm^{-1}K^{-1}$ at ~300K)[35] that plays an important role in lowering the heat flow. Therefore, the cotton wool fibres can be considered as empty spaces in the material filled with air as the thermal conductivities are comparable (thermal conductivity of the air is about ~0.026 $Wm^{-1}K^{-1}$ at ~300 K)[2].

Another important aspect that has a major contribution in lowering thermal flux through these **CW1** and **CW2** pellets is the very low mass of graphite existing in them. To be specific, in **CW1** pellet, the estimated graphite mass is only about 0.0175 g (estimated using the total graphite mass that was loaded into the cotton wool ball) and it is further low in **CW2** pellet, which is about 0.0147 g, these masses are smaller than the graphite mass (0.125 g) that was used to make a complete graphite pellet. Therefore, the amount of graphite consumed in **CW1** and **CW2** are only about 14% and 11.7% of the mass that was used to make a graphite pellet of similar dimension, respectively. Further, the density of the graphite pellet used in this work was estimated using its mass/volume ratio and it was about 1.9 gcm^{-3}. But, the graphite densities in **CW1** and **CW2** pellets were about 0.285 gcm^{-3} and 0.234 gcm^{-3},

respectively, which are about 7 to 8 times smaller than graphite pellet and thus these can be called as low-density graphite pellets (Figure 4 (d)).

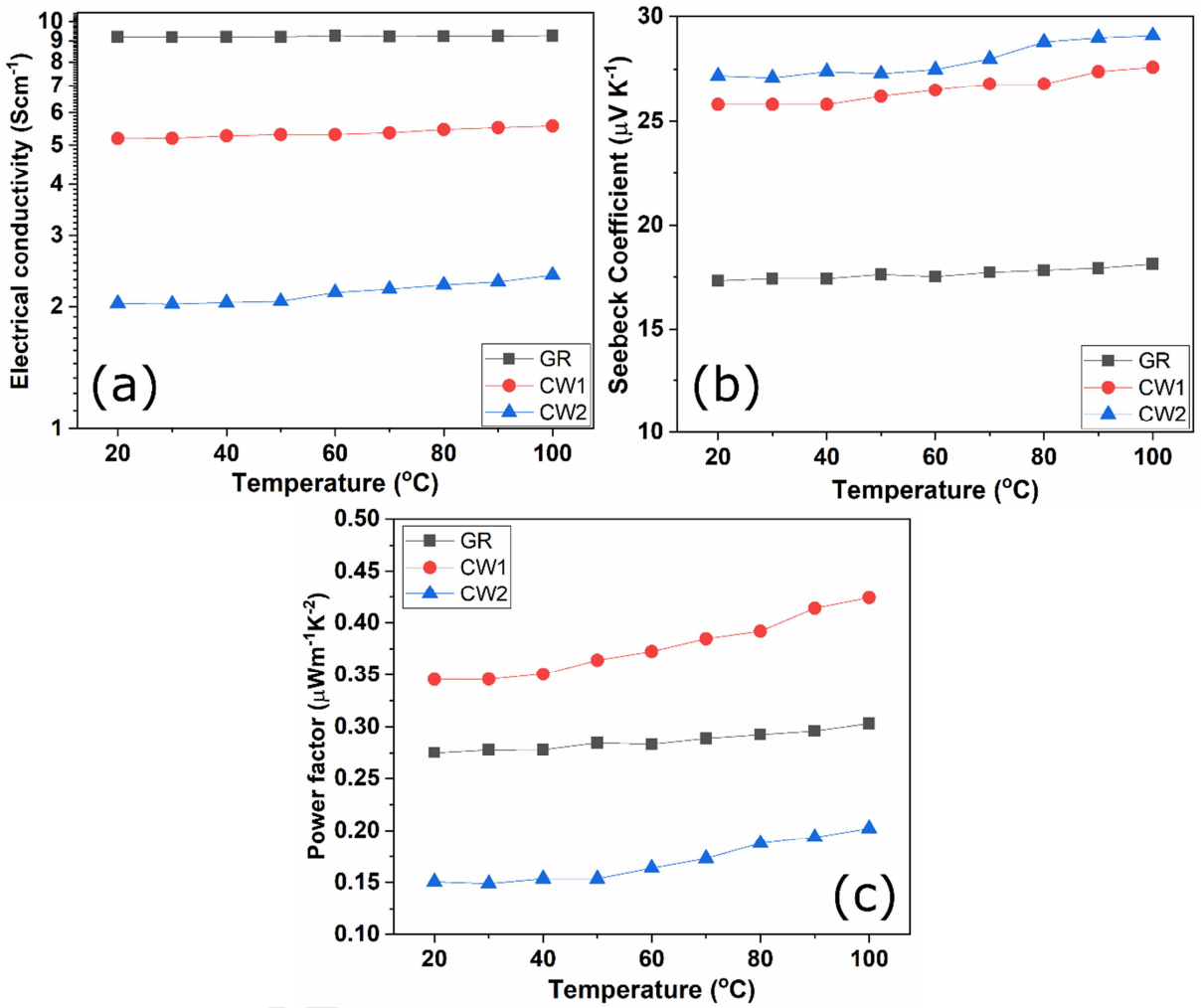

Figure 5. Temperature-dependent (a) electrical conductivity, (b) Seebeck coefficient, and (c) thermoelectric power factors of graphite (**GR**), **CW1**, and **CW2** samples.

Electrical conductivity data is shown in Figure 5 (a) reveals that higher levels of porosity led to lower electrical conductivity. The measured room temperature conductivity values of graphite, **CW1**, and **CW2** pellets are 9.18 Scm^{-1}, 5.18 Scm^{-1}, and 2.03 Scm^{-1}, respectively. The observed electrical conductivity of graphite pellet appears to be almost same with an increase in temperature. For **CW1** and **CW2** pellets, the conductivity found to increase with a small value as a function of temperature. The measured Seebeck coefficient data for all the samples are shown in Figure 5 (b). The observed Seebeck coefficient of

graphite found to be almost constant as a function of temperature with a small increase from 17.3 μVK^{-1} at room temperature to 18.1 μVK^{-1} at 100 ºC. In case of **CW1** and **CW2**, the Seebeck values are improved as compared to graphite pellet with room temperature values of 25.8 μVK^{-1} and 27.2 μVK^{-1}, which are further increased to 27.6 μVK^{-1} and 29.1 μVK^{-1}, respectively at 100 ºC. These changes in the electrical conductivity of **CW1** and **CW2** could be attributed to scattering of electrical charge carriers because of more interfaces between the graphitic structures leading to decrease in the number of effective charge carriers that contribute to the electrical conductivity. The resultant power factors ($S^2\sigma$) are estimated using the above data of electrical conductivity and Seebeck coefficient, shown in Figure 5 (c). The power factor of **CW1** is observed to be more than pure graphite pellet reaching a maximum value of about 0.424 $\mu Wm^{-1}K^{-2}$ at 100 ºC. The maximum values for graphite and **CW2** pellets are about 0.303 $\mu Wm^{-1}K^{-2}$ and 0.201 $\mu Wm^{-1}K^{-2}$, respectively. The decrease in power factor in case of **CW2** is indeed due to its low electrical conductivity as compared to the other two. The improved value in **CW1** shows the possibility of changing thermoelectric properties without playing with material's chemistry. It was found that the observed power factors of low graphite-loaded pellets, **CW3** and **CW4** are 0.09 $\mu Wm^{-1}K^{-2}$ and 0.05 $\mu Wm^{-1}K^{-2}$ respectively, which are very low as compared to **CW1** or **CW2**. The Seebeck coefficient, electrical conductivity and power factors of all the samples observed at 100 ºC are summarized in Figure S2 of the Supplementary material. The reason behind the decreased electrical conductivity in these pellets is the minimum graphitic content in the pellets hence less conducting paths for the charge carriers. The amount of graphite in **CW3** and **CW4** are lower than previous ones, which were about 10.5% and 9.0% respectively with respect to the graphite pellet.

The observed power factor of **CW1** is comparable to carbon nanotube (CNT) foam prepared by rapid solvent evaporation method which produced power factors of 0.43-0.73

$\mu Wm^{-1}K^{-2}$ (Seebeck coefficient = 32 to 34 μVK^{-1}, electrical conductivity = 4.02 to 6.58 S cm^{-1}) at room temperature.[36] Similarly, the pristine 3D CNT network fabricated using chemical vapour deposition (CVD) has shown the Seebeck coefficient and electrical conductivity of 27 μVK^{-1} and 150 S m^{-1} respectively, producing a power factor of 0.11 $\mu Wm^{-1}K^{-2}$ at 600 K.[37] So, the present method for making porous graphite pellets can result in similar performance along with economical and green fabrication process.

It is proposed that by carefully controlling the level of porosity in a material, the electrical and thermal properties can be modified. This approach can also works for other materials that are electrically good conductors as the electrical conductivity always deteriorates due to decreased connections between the conducting particles/grains. As the cotton wool cannot withstand at higher temperatures, the materials can be used for low-grade heat conversion applications. By cautiously analysing materials property at different porosity levels, low thermal conductivity and improved power factors can be achieved simultaneously.

4. Conclusions

A new and green method to make low-density and solid graphite pellets was achieved at ambient conditions. The improvements in the thermal properties of the low-density graphite pellets were observed as compared to bulk graphite pellet. The mechanical properties of the pellets are quite good as compared to the completely porous carbon 3D foams or porous solids as the porous pellets in the present work are already pressed with 2 ton of load. So, the pellets can be suitable for the solid state devices as long as they are used within a safe temperature limit. It is proposed that the method can be successfully extended to other materials to get better thermoelectric performances.

Acknowledgments

Authors are thankful to the Welsh Government (EU European Regional Development Fund) for funding the RICE (Reducing Industrial Carbon Emission) project (Grant Number: 81435). Authors would like to acknowledge the assistance provided by Swansea University College of Engineering AIM Facility, which was funded in part by the EPSRC (EP/M028267/1), the European Regional Development Fund through the Welsh Government (80708) and the Ser Solar project via Welsh Government.

Conflict of interests

The authors declare that there are no conflict of interests.

References

[1] R. Mulla, C.W. Dunnill, Powering the Hydrogen Economy from Waste Heat: A Review of Heat-to-Hydrogen Concepts, ChemSusChem, 12 (2019) 3882-3895.
[2] H.J. Goldsmid, Porous Thermoelectric Materials, Materials (Basel), 2 (2009) 903-910.
[3] B. Xu, T. Feng, M.T. Agne, L. Zhou, X. Ruan, G.J. Snyder, Y. Wu, Highly Porous Thermoelectric Nanocomposites with Low Thermal Conductivity and High Figure of Merit from Large-Scale Solution-Synthesized Bi2Te2.5Se0.5 Hollow Nanostructures, Angewandte Chemie International Edition, 56 (2017) 3546-3551.
[4] R. Mulla, M.H.K. Rabinal, Copper Sulfides: Earth-Abundant and Low-Cost Thermoelectric Materials, Energy Technology, 7 (2019) 1800850.
[5] P. Giulia, Thermoelectric materials: The power of pores, Nature Reviews Materials, 2 (2017) 17006.
[6] B. Xu, T. Feng, Z. Li, S.T. Pantelides, Y. Wu, Constructing Highly Porous Thermoelectric Monoliths with High-Performance and Improved Portability from Solution-Synthesized Shape-Controlled Nanocrystals, Nano Letters, 18 (2018) 4034-4039.
[7] X. Qi, Y. Huang, D. Wu, B. Jiang, B. Zhu, X. Xu, J. Feng, B. Jia, Z. Shu, J. He, Eutectoid nano-precipitates inducing remarkably enhanced thermoelectric performance in (Sn1−xCdxTe)1−y(Cu2Te)y, Journal of Materials Chemistry A, 8 (2020) 2798-2808.
[8] L. Li, Y. Liu, J.Y. Dai, H.X. Zhu, A.J. Hong, X.H. Zhou, Z.F. Ren, J.M. Liu, Thermoelectric property studies on CuxBi2SeS2 with nano-scale precipitates Bi2S3, Nano Energy, 12 (2015) 447-456.
[9] D.L. Medlin, G.J. Snyder, Interfaces in bulk thermoelectric materials: A review for Current Opinion in Colloid and Interface Science, Current Opinion in Colloid & Interface Science, 14 (2009) 226-235.
[10] S. Ohno, U. Aydemir, M. Amsler, J.-H. Pöhls, S. Chanakian, A. Zevalkink, M.A. White, S.K. Bux, C. Wolverton, G.J. Snyder, Achieving zT > 1 in Inexpensive Zintl Phase Ca9Zn4+xSb9 by Phase Boundary Mapping, Advanced Functional Materials, 27 (2017) 1606361.
[11] X. Chen, F. Cai, C. Liu, R. Dong, L. Qiu, L. Jiang, G. Yuan, Q. Zhang, Enhanced Thermoelectric Performance of Bi2Te2.7Se0.3/Bi2S3 Synthesized by Anion Exchange Method, physica status solidi (RRL) – Rapid Research Letters, n/a (2020) 1900679.

[12] L. You, Y. Liu, X. Li, P. Nan, B. Ge, Y. Jiang, P. Luo, S. Pan, Y. Pei, W. Zhang, G.J. Snyder, J. Yang, J. Zhang, J. Luo, Boosting the thermoelectric performance of PbSe through dynamic doping and hierarchical phonon scattering, Energy & Environmental Science, 11 (2018) 1848-1858.
[13] R. Mulla, M.K. Rabinal, Ambient growth of highly oriented Cu2S dendrites of superior thermoelectric behaviour, Applied Surface Science, 397 (2017) 70-76.
[14] J.-F. Li, W.-S. Liu, L.-D. Zhao, M. Zhou, High-performance nanostructured thermoelectric materials, NPG Asia Materials, 2 (2010) 152-158.
[15] S. Ghosh, I. Calizo, D. Teweldebrhan, E.P. Pokatilov, D.L. Nika, A.A. Balandin, W. Bao, F. Miao, C.N. Lau, Extremely high thermal conductivity of graphene: Prospects for thermal management applications in nanoelectronic circuits, Applied Physics Letters, 92 (2008) 151911.
[16] A.S. Nissimagoudar, N.S. Sankeshwar, Significant reduction of lattice thermal conductivity due to phonon confinement in graphene nanoribbons, Physical Review B, 89 (2014) 235422.
[17] S.S. Kubakaddi, K.S. Bhargavi, Enhancement of phonon-drag thermopower in bilayer graphene, Physical Review B, 82 (2010) 155410.
[18] C.N.R. Rao, K. Biswas, K.S. Subrahmanyam, A. Govindaraj, Graphene, the new nanocarbon, Journal of Materials Chemistry, 19 (2009) 2457-2469.
[19] J. Xu, X. Zhou, M. Chen, S. Shi, Y. Cao, Preparing hierarchical porous carbon aerogels based on enzymatic hydrolysis lignin through ambient drying for supercapacitor electrodes, Microporous and Mesoporous Materials, 265 (2018) 258-265.
[20] R.M. Hodlur, M.K. Rabinal, Self assembled graphene layers on polyurethane foam as a highly pressure sensitive conducting composite, Composites Science and Technology, 90 (2014) 160-165.
[21] X.-C. Zhang, F. Scarpa, R. McHale, A.P. Limmack, H.-X. Peng, Carbon nano-ink coated open cell polyurethane foam with micro-architectured multilayer skeleton for damping applications, RSC Advances, 6 (2016) 80334-80341.
[22] J. Tang, J. Yang, X. Zhou, H. Yao, L. Zhou, A porous graphene/carbon nanowire hybrid with embedded SnO2 nanocrystals for high performance lithium ion storage, Journal of Materials Chemistry A, 3 (2015) 23844-23851.
[23] Y. Li, B. Shen, X. Pei, Y. Zhang, D. Yi, W. Zhai, L. Zhang, X. Wei, W. Zheng, Ultrathin carbon foams for effective electromagnetic interference shielding, Carbon, 100 (2016) 375-385.
[24] Y. Shi, G. Liu, R. Jin, H. Xu, Q. Wang, S. Gao, Carbon materials from melamine sponges for supercapacitors and lithium battery electrode materials: A review, Carbon Energy, 1 (2019) 253-275.
[25] Y. Wei, H. Liu, S. Liu, M. Zhang, Y. Shi, J. Zhang, L. Zhang, C. Gong, Waste cotton-derived magnetic porous carbon for high-efficiency microwave absorption, Composites Communications, 9 (2018) 70-75.
[26] N.L. Teradal, S. Marx, A. Morag, R. Jelinek, Porous graphene oxide chemi-capacitor vapor sensor array, Journal of Materials Chemistry C, 5 (2017) 1128-1135.
[27] Y. Chen, X. Li, K. Park, J. Song, J. Hong, L. Zhou, Y.-W. Mai, H. Huang, J.B. Goodenough, Hollow Carbon-Nanotube/Carbon-Nanofiber Hybrid Anodes for Li-Ion Batteries, Journal of the American Chemical Society, 135 (2013) 16280-16283.
[28] Y. Chen, Z. Lu, L. Zhou, Y.-W. Mai, H. Huang, Triple-coaxial electrospun amorphous carbon nanotubes with hollow graphitic carbon nanospheres for high-performance Li ion batteries, Energy & Environmental Science, 5 (2012) 7898-7902.
[29] J.C. Bear, J.D. McGettrick, I.P. Parkin, C.W. Dunnill, T. Hasell, Porous carbons from inverse vulcanised polymers, Microporous and Mesoporous Materials, 232 (2016) 189-195.
[30] R.T. Woodward, F. Markoulidis, F. De Luca, D.B. Anthony, D. Malko, T.O. McDonald, M.S.P. Shaffer, A. Bismarck, Carbon foams from emulsion-templated reduced graphene oxide polymer composites: electrodes for supercapacitor devices, Journal of Materials Chemistry A, 6 (2018) 1840-1849.
[31] R. Zeng, H. Deng, Y. Xiao, J. Huang, K. Yuan, Y. Chen, Cross-linked graphene/carbon nanotube networks with polydopamine “glue” for flexible supercapacitors, Composites Communications, 10 (2018) 73-80.

[32] H. Xu, Z. Zeng, Z. Wu, L. Zhou, Z. Su, Y. Liao, M. Liu, Broadband dynamic responses of flexible carbon black/poly (vinylidene fluoride) nanocomposites: A sensitivity study, Composites Science and Technology, 149 (2017) 246-253.
[33] H. Jin, L. Zhou, C.L. Mak, H. Huang, W.M. Tang, H.L.W. Chan, High-performance fiber-shaped supercapacitors using carbon fiber thread (CFT)@polyanilne and functionalized CFT electrodes for wearable/stretchable electronics, Nano Energy, 11 (2015) 662-670.
[34] R. Mulla, C.W. Dunnill, An Easy Operational Tool to Evaluate Seebeck Coefficient, Instrument and measurement, Submitted Feb 2020 (2020).
[35] A. Abbas, Y. Zhao, J. Zhou, X. Wang, T. Lin, Improving thermal conductivity of cotton fabrics using composite coatings containing graphene, multiwall carbon nanotube or boron nitride fine particles, Fibers and Polymers, 14 (2013) 1641-1649.
[36] M.-H. Lee, Y.H. Kang, J. Kim, Y.K. Lee, S.Y. Cho, Freely Shapable and 3D Porous Carbon Nanotube Foam Using Rapid Solvent Evaporation Method for Flexible Thermoelectric Power Generators, Advanced Energy Materials, 9 (2019) 1900914.
[37] J. Chen, X. Gui, Z. Wang, Z. Li, R. Xiang, K. Wang, D. Wu, X. Xia, Y. Zhou, Q. Wang, Z. Tang, L. Chen, Superlow Thermal Conductivity 3D Carbon Nanotube Network for Thermoelectric Applications, ACS Applied Materials & Interfaces, 4 (2012) 81-86.

Graphite-Loaded Cotton Wool: A Green Route to Highly-Porous and Solid Graphite Pellets for Thermoelectric Devices

Rafiq Mulla and Charles W. Dunnill*

Energy Safety Research Institute, Swansea University, Bay Campus, Fabian Way, SA1 8EN, UK.

Highlights:

- A green and direct method for making highly porous yet solid graphite pellets has been presented.
- Significant reduction in the thermal conductance in porous pellets has been observed.
- The work can re-stimulate the use of porous graphite for thermoelectric applications.

Declaration of interests

☒ The authors declare that they have no known competing financial interests or personal relationships that could have appeared to influence the work reported in this paper.

☐The authors declare the following financial interests/personal relationships which may be considered as potential competing interests: